Performance optimization of a chitosan/anammox reactor in nitrogen removal from synthetic wastewater in the presence of metals

Amin Mojiri[a], John L. Zhou[b], Akiyoshi Ohashi[a], Noriatsu Ozaki[a], Yoshiteru Aoi[c], Mohammadtaghi Vakili[d], Tomonori Kindaichi[a,*]

[a]Department of Civil and Environmental Engineering, Graduate School of Advanced Science and Engineering, Hiroshima University, 1-4-1 Kagamiyama, Higashihiroshima 739-8527, Japan; amin.mojiri@gmail.com (A.Mojiri), ecoakiyo@hiroshima-u.ac.jp (A. Ohashi), ojaki@hiroshima-u.ac.jp (N. Ozaki)

[b]Center for Green Technology, School of Civil and Environmental Engineering, University of Technology Sydney, 15 Broadway, NSW 2007, Australia; JunLiang.Zhou@uts.edu.au (J.L. Zhou)

[c]Program of Biotechnology, Graduate School of Integrated Sciences for Life, Hiroshima University, 1-3-1 Kagamiyama, Higashihiroshima, 739-8530, Japan; yoshiteruaoi@hiroshima-u.ac.jp (Y. Aoi)

[d]Green intelligence Environmental School, Yangtze Normal University, Chongqing, 408100, China; mvakili1981@yahoo.com (A. Vakili)

*Corresponding Author: Email: tomokin@hiroshima-u.ac.jp

Highlights:

- Integrated chitosan/anammox showed a good performance in removing nitrogen from wastewater.
- At optimum performance, 90.8% of ammonia and 83.5% of nitrite were removed by chitosan/anammox.
- Anammox attached to the surface of chitosan which was shown by microscope images.
- Adding 7 mg/L of Fe and Cu inhibited anammox activity.

Figures

Figure 1: Inoculation process of anammox bacteria in the first reactor.

Figure 2: Designed reactors in the current study.

Figure 3: A FISH image of the inoculum with Alexa Fluor 488-labelled probe EUB338mix (green) and Alexa Fluor 555-labelled Amx368 probe (red). Anammox bacteria appear as yellow. The scale bar represents 10 µm.

Figure 4: Performance of the first reactor: (A) Nitrogen loading and removal rates, (B) removal efficiency, and (C) concentration.

Figure 5: Performance of the second reactor: (A) Nitrogen loading and removal rates, (B) removal efficiency, and (C) concentration.

Figure 6: Figure 6: Attachment of anammox on chitosan.

Pink color in chitosan indicates the attached anammox bacteria

Figure 7: 3D surface plots for the removal of (A) ammonia, (B) nitrite, and (C) total nitrogen (TN) via the first reactor.

Figure 8: 3D surface plots for the removal of (A) ammonia, (B) nitrite, and (C) total nitrogen (TN) via the second reactor

Figure 9: Removal efficiency of the (A) first reactor and (B) second reactor.

Abstract: Anaerobic ammonia oxidation (anammox) is an environmentally friendly, cost-effective, and biological method for nitrogen treatment from aqueous solutions. However, anammox activity can be affected by other contaminants such as metals. Thus, in this study, anammox was attached to chitosan to reduce the negative impacts of contaminants on its performance. Two reactors comprising chitosan and anammox bacteria (first reactor, chitosan/anammox) and solely anammox (second reactor, control) were run for 73 d. The nitrogen loading rate (NLR) varied from 2 to 14 gN/(L d), while the nitrogen concentration varied from 80 to 700 mg/L. The chitosan/anammox reactor showed a better performance than the sole anammox control, with respective maximum abatement values of ammonia (NH_4^+), nitrite (NO_2^-), and total nitrogen (TN) of 90.8, 83.5, and 81.7% on days 20 to 25 under an NLR of 8–10 kgTN/(m^3 d). Response surface methodology (RSM) was employed to optimize the performance of both reactors, and a reasonable R^2 value showed that the RSM well optimized the performance of the reactors. After finding the optimum performance conditions for both reactors, Fe and Cu (0.5–7.0 mg/L) were added to the influent. The performance of both reactors decreased to 0% following the addition of 7.0 (first reactor) and 6.5 (second reactor) mg/L Cu and Fe, respectively. This indicated that chitosan not only enhanced nitrogen removal by anammox but also improved the resistance of anammox to metals.

Keywords: Anammox, Chitosan, Heavy Metals, Wastewater

1. Introduction

Nitrogen contamination (such as ammonia) has been considered a serious environmental issue because it may cause eutrophication, a toxic problem to aquatic environments [1]. In conventional wastewater treatment systems, aeration and organic carbon sources are required to complete heterotrophic denitrification, which increases the treatment costs, while residual organic matter in the effluent causes secondary contamination [2]. Anaerobic ammonia oxidation (anammox) is a promising biological technology to remove nitrogen from aqueous solution [3]. The principle of the anammox process comprises the application of NO_2^--N as the electron acceptor and oxidation of NH_4^+-N to nitrogen gas by anaerobic ammonium oxidizing bacteria [4,5], as shown in equation 1:

$$NH_4^+ + 1.32NO_2^- + 0.06HCO_3^- + 0.13H^+ \longrightarrow 1.02N_2 + 0.26NO_3^- + 0.06CH_2O_{0.5}N_{0.15} + 2.03H_2O \quad \text{(eq. 1)}$$

Anammox is a cost-effective alternative nitrogen treatment method, which requires approximately 60% less aeration than conventional nitrification/denitrification procedures and does not require organic carbon [6,7]. Among the five known genera of anammox bacteria, four are mainly found in freshwater, including: *Candidatus Jettenia*, *Ca. Brocadia*, *Ca. Anammoxoglobus*, and *Ca. Kuenenia* [8]. In this study, we used *Ca. Jettenia* and *Ca. Brocadia* as both genera have already been employed to treat wastewater. Indeed, Liu et al. [9] and Mojiri et al. [10] applied *Ca. Brocadia* and *Ca. Jettenia* in a sequencing batch reactor and hybrid reactor. The main drawbacks of anammox bacteria include a slow growth rate, reduced anammox activity in the presence of high amounts of NO_2^- and ammonia, and low resistance against other contaminants such as metals [11]. Zhang et al. reported that as a single method, anammox removed less than 40% ammonia [12]. Moreover, heavy metals are widely found in

List of Abbreviations: Annamox, anaerobic ammonia oxidation; CCD, central composite design; FISH, fluorescence in situ hybridization; HRT, hydraulic retention time; MLSS, mixed liquor suspended solids; NLR, nitrogen loading rate; PVA-SA, poly (vinyl alcohol)-sodium alginate; RSM, response surface methodology; TN, total nitrogen; USB, upflow sludge blanket;

wastewater [13] of which some, such as iron and copper, have toxic effects on anammox activity and inhibit nitrogen removal [14]. Therefore, researchers have attempted to improve the growth and resistance of anammox bacteria, in terms of improving the microbial community, by using various hybrid processes and systems. To achieve this goal, in the current study, anammox was integrated with chitosan. Chitosan improves the microbial community and removes pollutants via adsorption. Indeed, Yapsakli et al. employed a hybrid reactor, which included ammonium adsorption, to obtain a stable effluent nitrogen amount and eliminate approximately 95% of the nitrogen in wastewater [15].

Chitosan is one of the most common biopolymers and is found in the shells of crustaceans, such as shrimp [16]. Its structure contains amino (NH_2^-), hydroxyl (OH^-), and other reactive functional groups [17]. Chitosan has various environmental advantages, such as non-toxicity, biocompatibility, and biodegradability [18], and has therefore been applied in various wastewater treatment studies. Indeed, using a chitosan-based adsorbent, Yang et al. [19] removed copper from wastewater, while Gao and Zhang [17] removed ammonia from an aqueous solution. Additionally, Torres et al. [20] reported that chitosan improves the microbial communities and enhances the growth of bacteria during anaerobic treatment of wastewater.

Thus, the main goal of the study was to attach anammox bacteria to the chitosan surface to improve the bacterial community and increase its resistance to metals. Notably, to the best of our knowledge, no such designed technique has been reported in the literature to date. Additionally, the treatment performance was optimized by response surface methodology (RSM).

2. Materials and Methods

2.1. Anammox/chitosan reactor and experimental description

Two 100 mL reactors were run for 73 d [21]. The first reactor (chitosan/anammox) was occupied with chitosan from crab shells (small flakes) and then inoculated with anammox bacteria (Figure 1), including *Candidatus Brocadia* and *Ca. Jettenia caeni* granules, which were obtained from an upflow reactor in our laboratory. The DNA extraction process of the biomass is illustrated in Table A.1 (supplementary file extracted from our previous study [10]). After inoculation, the concentration of the mixed liquor suspended solids (MLSS) was approximately 200 mg/L [15]. The second reactor (anammox) was inoculated with anammox bacteria, including *Ca. Brocadia* and *Ca. Jettenia caeni* granules. Both reactors were circulated for two days, to settle the bacteria, and operated in upflow mode. The experiment was performed at 24 ± 2 °C, and both reactors (Figure 2) were flushed with nitrogen gas. The system running conditions are listed in Table 1. The average hydraulic retention time (HRT) was approximately 1.2 h, based on preliminary experiments. Okamoto et al. [21] fixed the HRT at 1 h, which is similar to the HRT employed in our current study.

Figure 1: Inoculation process of anammox bacteria in the first reactor (chitosan/anammox)

Table 1: Fixed conditions during the reactor runs

Figure 2: Designed reactors in the current study

2.2. Synthetic wastewater

Wastewater was synthesized with a composition of 40–350 mg/L NH_4^+-N (ammonia), 40–350 mg/L NO_2^-–N (nitrite), 0.2 mM KH_2PO_4, 1 g/L $KHCO_3$, 1.2 mM $MgSO_4 \cdot 7H_2O$, 1.2 mM $CaCl_2 \cdot 2H_2O$ [10], and 1 mL of trace element solutions I and II, as explained by Awata et al. [22]. HCl or NaOH were employed to maintain a neutral pH. To determine the effect of metals on anammox activity, $FeCl_3$ and $CuCl_2.2H_2O$ were used to attain Fe and Cu values in the range 0.5–7.0 mg/L. Wang et al. [23] studied anammox activity under Fe(III) supplementation and employed $FeCl_3$ to reach the Fe(III) concentration, which is in line with the method used in the current study. Notably, Mak et al. [24], $FeSO_4$ and $CuSO_4$ were added to reach the required Fe and Cu concentrations; however, we used $FeCl_3$ and $CuCl_2$ owing to the presence of SO_4 in the employed synthetic wastewater. This is because a high amount of SO_4 can reduce the anammox activity [25].

2.3. Analytical methods

The standard method reported in the literature [26] was considered for testing the wastewater. The pH and temperature (°C) were monitored using a Navi F-52 pH meter (Horima Co. Ltd., Kyoto, Japan). Ammonia, NO_3^-, and NO_2^- were analyzed via ion-exchange chromatography (HPLC 20A, Shimadzu Co. Ltd., Kyoto, Japan), while Cu and Fe were analyzed with a Hach DR2800 spectrophotometer (Hach Co. Ltd., Loveland, CO, USA).

2.4. Fluorescence in situ hybridization (FISH)

FISH images of the inoculated biomass samples were observed with an Axioimager M1 epifluorescence microscope (Carl Zeiss, Oberkochen, Germany) as described by Kindaichi et al. [27]. In this case, EUB338mix probes labeled with Alexa Fluor 488 were employed to observe most bacteria, while an Amx368 probe labeled with Alexa Fluor 555 was employed to observe the anammox bacteria.

2.5. Optimization by RSM

Contaminant abatement effectiveness was estimated based on the initial and final concentrations using equation 2:

$$Removal\ (\%) = \frac{(C_i - C_f)100}{C_i} \qquad \text{(eq. 2)}$$

where the initial and final concentrations are indicated by C_i and C_f, respectively.

Statistical analysis and optimization were performed to remove the total nitrogen (TN), nitrite (NO_2^--N), and ammonia (NH_4^+-N) via RSM. Two independent factors, namely time and nitrogen loading rate (NLR), over the central composite design (CCD) with three replications of factorial points were considered. The two effectual variables were assessed at three levels: low (−1), central (0), and high (+1). A quadratic model that also comprised the linear model (equation 3) was applied, whereby values of "Prob > F" less than 0.05 indicated that the model terms were significant. The desirability graphs are presented in Figures A.3 and A.4 in the appendix.

$$Y = \beta_0 + \sum_{j=1}^{k} \beta_j X_j + \sum_{j=1}^{k} \beta_{jj} X_j^2 + \sum_i \sum_{j=2}^{k} \beta_{ij} X_i X_j + e \quad \text{(eq. 3)}$$

where *Y* defines the responses; X_i and X_j are variables; β_0 represents the fixed coefficient; β_j, β_{jj}, and β_{ij}, are the interface coefficients of the linear, quadratic, and second-order terms, respectively; *k* highlights the quantity of factors; and *e* marks the error.

2.6. Adsorption isotherm

Batch experiments for the adsorption study were run using different dosages (up to 8 g/L) of chitosan in fixed ammonia, Fe and Cu concentration (4.0 mg/L), and adsorption time (1 h) at neutral pH. Beakers with working volumes of 100 mL were shaken at 100 rpm for 1 h. The adsorption capacity (mg/g) was assessed using equation 4:

$$q_e = \frac{(C_0 - C_{eq})V}{m_s} \quad \text{(eq. 4)}$$

where q_e is the initial pollutant concentration; C_{eq} is the ammonia, Fe, or Cu concentration (mg/L) at equilibrium; *V* is the solution volume (L); and m_s represents the mass of the adsorbent (g).

3. Results and Discussion

Two reactors were operated in this study. The first reactor was filled with chitosan as a fixed-bed column and inoculated with anammox bacteria. The microbial communities are shown in Table A.1. Approximately 41.4% of *the* microbial community contained the *Planctomycetes Ca. Brocadia* and *Ca. Jettenia*. Therefore, the reactors mainly comprised these two types of anammox bacteria. In addition, *Chlorobia* (13.61%) and *Chloroflexi* (15.56%) bacteria occupied a significant part of the inoculated biomass. Casagrande et al. [28] reported that there are usually some groups of bacteria that coexist with anammox bacteria; however, generally, these do not have any significant effect on the nitrogen removal process. FISH was conducted to verify the presence of anammox bacteria in the biomass (Figure 3), clearly revealing that most parts of the inoculate biomass comprised anammox bacteria.

The operation of both reactors consisted of three phases, namely, (a) Phase 1: 0–24, (b) Phase 2: 25–48, and (c) Phase 3: 49–73 d. The NLR gradually increased from 2 to 14 kgTN/(m^3 d) in phases 1 and 2. Subsequently, during phase 3, the nitrogen removal performance decreased, thereby leading to a decrease in the NLR to 2–8 kgTN/(m^3 d).

Figure 3: Fluorescence in situ hybridization **(**FISH) image of the inoculum using Alexa Fluor 488 labeled EUB338 mix (green) and Alexa Fluor 555 labeled Amx368 (red) probes. Anammox bacteria appear as yellow. Scale bar represents 10 µm.

3.1. Removal of nitrogen compounds

The nitrogen removal performances of the first and second reactors are displayed in Figures 4 and 5, respectively. In the first reactor (chitosan/anammox), the respective maximum abatement values of ammonia and total nitrogen (TN) were 90.8 and 81.7% during day 25, with an NLR of 10.0 kgTN/(m^3 d). In addition, maximum nitrite elimination (83.5%) was observed during day 20 with an NLR of 8.0 kgTN/(m^3 d). Minimum elimination of ammonia and nitrite (64.2 and 63.8%, respectively) was observed during day 48, with an NLR of 14.0 (kgTN/(m^3 d), while minimum TN elimination was achieved during day 44 with an NLR of 14 kgTN/(m^3 d).

In the second reactor (solely anammox), maximum elimination of ammonia (71.0%) and TN (63.2%) was achieved during day 20 with an NLR of 8.0 kgTN/(m^3 d). Maximum nitrite removal (71.4%) was observed during day 24 with an NLR also equal to 8.0 kgTN/(m^3 d). In contrast with the maximum removal effectiveness, the minimum elimination of nitrite and TN, were 59.3 and 51.6%, respectively, during day 48 with an NLR of 14.0 kgTN/(m^3 d). Minimum TN elimination was achieved during day 40 with an NLR of 13.5 kgTN/(m^3 d), while minimum ammonia abatement (59.6%) was observed during day 44 with an NLR of 14 kgTN/(m^3 d).

Figure 4: Performance of the first reactor: (A) Nitrogen loading and removal rates, (B) removal efficiency, and (C) concentration.

Figure 5: Performance of the second reactor: (A) Nitrogen loading and removal rates, (B) removal efficiency, and (C) concentration.

Agustina et al. [29] removed approximately 74% nitrogen during optimum performance with anammox, at temperatures in the range 25–27 °C, during day 178, in an upflow reactor. In addition, maximum nitrogen removal (75%) by a modified partial nitrification-anammox reactor at 35 °C was reported by Han et al. [30]. Tuyen et al. [31] removed approximately 60% nitrogen using an anammox procedure with a poly (vinyl alcohol)-sodium alginate (PVA-SA) gel bed. Notably, the removal performance of our second reactor approximately equaled those reported in these three studies. Moreover, the results in our present study clearly revealed that the removal efficiencies of ammonia, TN, and nitrite in the first reactor were significantly higher than those observed in the second reactor. This higher removal performance was attributed to the attachment of anammox to chitosan (Figure 6). One reason for this is the ability of chitosan to remove ammonia and nitrite from wastewater. Hudayah et al. [32] stated that using chitosan could improve the microbial community and anaerobic granule quality during simultaneous microbial adaptation and granulation. Furthermore, fast microbial aggregation using chitosan was reported by Yang et al. [33], while the improvement of biomass and sludge granularity in an upflow sludge blanket (USB) reactor was reported by Torres et al. [20]. Patil et al. [34] removed more than 50% nitrate from groundwater by chitosan, while de Luna et al. [35] reported up to 67.5% ammonia removal from an aqueous solution by chitosan. On the other hand, the improvement of the microbial community due to the presence of chitosan might also result in an improvement in the performance of the first reactor (chitosan/anammox) over that of the second reactor.

Figure 6: Attachment of anammox on chitosan.

Pink color in chitosan indicates the attached anammox bacteria

Next, we employed RSM and CCD to optimize and simulate nitrogen removal via the first and second reactors. The 3D plots for the abatement of ammonia, nitrite, and TN, based on the RSM for the first and second reactors, are shown in Figures 7 and 8, respectively. As shown in Tables 2 and 3, the optimum abatement values of ammonia (89.3%), nitrite (79.6%), and TN (76.5%) were achieved at the optimal NLR of 9.6 kgTN/(m^3 d), after 14.5 d, for the first reactor. On the other hand, for the second reactor, the optimum abatement values of ammonia (68.7%), nitrite (78.3%), and TN (61.0%) were achieved at the optimal NLR of 7.7 kgTN/(m^3 d) after 33.8 d.

Table 2: Statistical analysis results for the response parameters in the response surface methodology (RSM)

Figure 7: 3D surface plots for the removal of (A) ammonia, (B) nitrite, and (C) total nitrogen (TN) via the first reactor.

Figure 8: 3D surface plots for the removal of (A) ammonia, (B) nitrite, and (C) total nitrogen (TN) via the second reactor.

Table 3: Removal efficiencies under optimum conditions

3.2. Effects of iron and copper on the anammox activity

Heavy metals can reach different water bodies from various industrial effluents [36]. Among the most common heavy metals, copper and iron are frequently present in industrial wastewaters [37], whereby Cu(II) and Fe(II) are essential micronutrients for microorganisms at low concentrations [38]. In this study, after determining the optimum performance of both reactors, the Fe(II) and Cu(II) concentrations were slightly increased (Table 4) in both reactors under optimum conditions.

Figure 9 illustrates the removal efficiencies of both reactors. In the first reactor, increasing Fe and Cu to 1 mg/L improved the removal effectiveness of ammonia (96.0%), nitrite (90.7%), and TN (87.9%). However, when the Fe and Cu concentrations were further increased from 1.5 to 5 mg/L, the abatement efficiencies decreased significantly to 50.3% (ammonia), 50.1% (nitrite), and 51.3% (for TN). Mojiri et al. [39] reported that the anammox performance is reduced in the presence of other contaminants, while Lotti et al. [40] reported that the anammox performance could be decreased by up to 50% on increasing the Cu concentration to 1.9 mg/L. For the second reactor, increasing the Fe and Cu concentrations to 1 mg/L enhanced the abatement efficiencies of ammonia (74.6%), nitrite (75.6%), and TN (69.2%). The abatement efficacy was dramatically decreased to 33.1% (for ammonia), 32.3% (for nitrite), and 30.8% (for TN).

The Fe and Cu concentrations were then decreased to 1 mg/L in both reactors. With this reduction in the Fe and Cu concentrations, the ammonia, nitrite, and TN removal efficiencies respectively increased again to 79.2, 77.2, and, 72.7% for the first reactor and 66.8, 65.3, 62.6% for the second reactor. These results show that the effects of Cu and Fe are reversible, since the reduction in the Fe and Cu concentrations improved the anammox activity. This is in agreement with the findings of Mak et al. [24] who also reported that the effects of Cu(II) on anammox bacteria during wastewater treatment are reversible.

With the increase in Fe and Cu concentrations to 7.0 and 6.5 mg/L, respectively, the performances of the first and second reactors both dropped to 0%. Liu and Ni [41] stated that a high concentration of Fe(II) might induce biomass destruction. The resistance of anammox bacteria against high concentrations of Fe and Cu in the first reactor was higher than that in the second reactor. This occurs because chitosan adsorbs Fe and Cu, and increases the microbial community. Rana et al. [42] also reported that heavy metals (such as copper and iron) can be removed by chitosan (extracted from crab shells).

Table 4: Addition of different concentrations of Fe and Cu in the reactors

Figure 9: Removal efficiency of the (A) first reactor and (B) second reactor.

3.3. Adsorption isotherm study

Batch experiments and adsorption isotherm studies were next conducted to better understand the functions of chitosan in ammonia, Fe, and Cu removal, since the first reactor was filled with chitosan. Table 5 shows important data attained from the Langmuir and Freundlich isotherm studies. These data reveal that Fe, Cu, and ammonia removal by chitosan is better explained by the latter isotherm. Thus, based on the Freundlich isotherm, the respective R^2, K_f, and n values were 0.85, 0.9, and 1.2 for Fe(II) elimination and 0.89, 5.3, and 2.7 for Cu(II) elimination. For ammonia removal, R^2, K_f, and n were 0.93, 16.2, and -3.1, respectively. The adsorption capacity (K_f; 0.05) and regression (R^2; 0.83) based on the Freundlich isotherm reported during Fe(II) removal via chitosan by Reiad et al. [43] are similar to those reported in our current study. Moreover, this group reported an R^2 value of 0.78 and b value of 0.35 during Fe(II) elimination using chitosan, based on the Langmuir isotherm [43], which are in line with the data from our current study. In a study on Cu removal by chitosan, K_f (13.2), n (2.1), and R^2 (0.83) were reported based on the Freundlich isotherm, and R^2 (0.84) was reported in terms of the Langmuir isotherm [18]. This approaches the findings of our current study.

Table 5: Langmuir and Freundlich isotherm studies for ammonia, Fe, and Cu removal by chitosan

4. Conclusions

Anammox activity can be reduced in the presence of other pollutants, such as metals. Therefore, in this study, we investigated chitosan/anammox integration. Two reactors, namely a first reactor comprising chitosan/anammox and a second reactor comprising anammox, were run for 73 d. After determining the optimum conditions to reach the maximum performance of the reactor, Fe and Cu were added to monitor the anammox activity in the presence of metals. The key findings of this study are as follows:

(1) The maximum abatement of ammonia, nitrite, and TN was 90.8, 83.5, and 81.7%, respectively, in the presence of chitosan/anammox.

(2) The maximum abatement of ammonia, nitrite, and TN was 71.0, 71.4, and 63.2%, respectively, in the sole presence of anammox.

(3) Optimization by RSM revealed that the optimum removal of ammonia (89.3%), nitrite (79.6%), and TN (76.5%) is reached at an optimal NLR of 9.6 kgTN/(m^3 d)] after 14.5 d for the chitosan/anammox reactor.

(4) Under optimum performance conditions, Fe and Cu were added into the influent to investigate the performance of the reactors in the presence of metals. Nitrogen abatement almost stopped after the addition of 7.0 mg/L Fe and Cu in the chitosan/anammox combination (first reactor) and after adding 6.5 mg/L Fe and Cu in the second reactor.

(5) Microscope images of the chitosan surface indicated that anammox bacteria were attached to the chitosan surface.

Acknowledgements:

Funding: This work was supported by JSPS KAKENHI grant number JP17F17375.

Conflict of Interest: The authors declare no conflicts of interest.

References

[1] J. Lin, P. Zhang, G. Li, J. Yin, J. Li, X. Zhao, Effect of COD/N ratio on nitrogen removal in a membrane-aerated biofilm reactor, Intern. Biodeterior. Biodegrad. 113 (2016) 74-79. https://doi.org/10.1016/j.ibiod.2016.01.009

[2] F. Cai, L. Lei, Y. Li, Rapid start-up of single-stage nitrogen removal using anammox and partial nitritation (SNAP) process in a sequencing batch biofilm reactor (SBBR) inoculated with conventional activated sludge, Intern. Biodeterior. Biodegrad. 147 (2020) 104877. https://doi.org/10.1016/j.ibiod.2019.104877

[3] L. Liu, M. Ji, F. Wang, Z. Yan, Z. Tian, Response of nitrogen removal performance, functional genes abundances and N-acyl-homoserine lactones release to carminic acid of anammox biomass, Bioresour. Technol. 299 (2020) 122567. https://doi.org/10.1016/j.biortech.2019.122567

[4] L. Lin, Y. Zhang, M. Beckman, W. Cao, T. Ouyang, S. Wang, Y.-Y. Li, Process optimization of anammox-driven hydroxyapatite crystallization for simultaneous nitrogen removal and phosphorus recovery, Bioresour. Technol. 290 (2019) 121779. https://doi.org/10.1016/j.biortech.2019.121779

[5] F. Xie, X. Ma, B. Zhao, Y. Cui, X. Zhang, X. Yue, Promoting the nitrogen removal of anammox process by Fe-C micro-electrolysis, Bioresour. Technol. 297 (2020) 122429. https://doi.org/10.1016/j.biortech.2019.122429

[6] S. Deng, Y. Peng, L. Zhang, L. Wu, Advanced nitrogen removal from municipal wastewater via two-stage partial nitrification-simultaneous anammox and denitrification (PN-SAD) process, Bioresour. Technol. 304 (2020) 122955. https://doi.org/10.1016/j.biortech.2020.122955

[7] H. Ma, Y. Xue, Y. Zhang, T. Kobayashi, K. Kubota, Y.-Y. Li, Simultaneous nitrogen removal and phosphorus recovery using an anammox expanded reactor operated at 25 °C, Water Res. 172 (2020) 115510. https://doi.org/10.1016/j.watres.2020.115510

[8] R. Schwartz-Narbonne, P. Schaeffer, E.C. Hopmans, M. Schenesse, E.A. Charlton, D. M. Jones, J.S.S. Damsté, M.F.U. Haque, M.S.M. Jetten, S.K. Lengger, J.C. Murrell, P. Normand, G.H.L. Nuijten, H.M. Talbot, D. Rush, A unique bacteriohopanetetrol stereoisomer of marine anammox, Org. Geochem. 143 (2020) 103994. https://doi.org/10.1016/j.orggeochem.2020.103994

[9] X. Liu, K. Arumugam, G. Natarajan, T.W. Seviour, D. Drautz-Moses, S. Wuertz, Y. Law, R.B.H. Williams, Draft genome sequence of a "*Candidatus Brocadia*" bacterium enriched from activated sludge collected in a tropical climate, Am. Sco. Microbiol. 6(19) (2018) e00406-e00418. https://doi.org/10.1128/genomeA.00406-18

[10] A. Mojiri, A. Ohashi, N. Ozaki, Y. Aoi, T. Kindaichi, Integrated anammox-biochar in synthetic wastewater treatment: Performance and optimization by artificial neural network, J. Clean. Prod. 243 (2020) 118638. https://doi.org/10.1016/j.jclepro.2019.118638

[11] A. Ziembińska-Buczyńska, A. Banach-Wiśniewska, M. Tomaszewski, I. Poprawa, S. Student, G. Cema, Ecophysiology and dynamics of nitrogen removal bacteria in a sequencing batch reactor during wastewater treatment start-up, Int. J. Environ. Sci. Technol. 16 (2019) 4215-4222. https://doi.org/10.1007/s13762-019-02275-w

[12] L. Zhang, P. Zheng, C.-j. Tang, J. Ren-cun, Anaerobic ammonium oxidation for treatment of ammonium-rich wastewaters, J. Zhejiang Univ. Sci. B. 9 (2008), 416-426. https://dx.doi.org/10.1631/jzus.B0710590

[13] H. Li, J. Watson, Y. Zhang, H. Lu, Z. Liu, Environment-enhancing process for algal wastewater treatment, heavy metal control and hydrothermal biofuel production: A critical

review, Bioresour. Technol. 298 (2020) 122421. https://doi.org/10.1016/j.biortech.2019.122421

[14] G.-F. Li, W.-J. Ma, Y.-F. Cheng, S.-T. Li, J.-W. Zhao, J.-P. Li, Q. Liu, N.-S. Fan, B.-C. Huang, R.-C. Jin, A spectra metrology insight into the binding characteristics of Cu^{2+} onto anammox extracellular polymeric substances, Chem. Eng. J. 393 (2020) 124800. https://doi.org/10.1016/j.cej.2020.124800

[15] K. Yapsakli, C.K. Aktan, B. Mertoglu, Anammox-zeolite system acting as buffer to achieve stable effluent nitrogen values, Biodegrad. 28 (2017) 69-79. https://doi.org/10.1007/s10532-016-9778-1

[16] C.G.D. Tovar, J. Delgado-Ospina, D.P.N. Porras, Y. Peralta-Ruiz, A.P. Cordero, J.I. Castro, M.N.C. Valencia, J.H. Mina, Colletotrichum gloesporioides inhibition in situ by Chitosan-Ruta graveolens essential oil coatings: Effect on microbiological, physicochemical, and organoleptic properties of guava (Psidium guajava L.) during room temperature storage, Biomol. 9 (2019) 399. https://doi.org/10.3390/biom9090399

[17] Y. Gao, J. Zhang, Chitosan modified zeolite molecular sieve particles as a filter for ammonium nitrogen removal from water, Int. J. Mol. Sci. 21 (2020) 2383. https://doi.org/10.3390/ijms21072383

[18] V. Rizzi, F. Romanazzi, J. Gubitosa, P. Fini, R. Romita, A. Agostiano, A. Petrella, P. Cosma, Chitosan film as eco-friendly and recyclable bio-adsorbent to remove/recover diclofenac, ketoprofen, and their mixture from wastewater, Biomol. 9 (2019) 571. https://doi.org/10.3390/biom9100571

[19] Z. Yang, Y. Chai, L. Zeng, Z. Gao, J. Zhang, H. Ji, Efficient removal of copper ion from wastewater using a stable chitosan gel material, Mol. 24 (2019) 4205. https://dx.doi.org/10.3390/molecules24234205

[20] K. Torres, F.J. Álvarez-Hornos, P. San-Valero, C. Gabaldón, P. Marzal, Granulation and microbial community dynamics in the chitosan-supplemented anaerobic treatment of wastewater polluted with organic solvents, Water Res. 130 (2018) 376-387. https://doi.org/10.1016/j.watres.2017.12.009

[21] H. Okamoto, K. Kawamura, T. Nishiyama, T. Fujii, K. Furukawa, Development of a fixed-bed anammox reactor with high treatment potential, Biodegrad. 24 (2013) 99-110. https://dx.doi.org/10.1007/s10532-012-9561-x

[22] T. Awata, Y. Goto, T. Kindaichi, N. Ozaki, A. Ohashi, Nitrogen removal using an anammox membrane bioreactor at low temperature, Water Sci. Technol. 72 (2015) 2148-2153. https://doi.org/10.2166/wst.2015.436

[23] X. Wang, D. Shu, H. Ye, Taxonomical and functional microbial community dynamics in an Anammox-ASBR system under different Fe (III) supplementation, Appl. Microbiol. Biotechno. 100 (2016), 10147-10163. https://doi.org/10.1007/s00253-016-7865-1

[24] C.Y. Mak, L. Jih-Gaw, M.J.K. Bashir, An overview of the effects of heavy metals content in wastewater on anammox bacteria, Adv. Environ. Stud. 2 (2018), 61-70. https://doi.org/10.36959/742/203

[25] E. Rikmann, I. Zekker, M. Tomingas, T. Tenno, A. Menert, L. Loorits, T. Tenno, Sulfate-reducing anaerobic ammonium oxidation as a potential treatment method for high nitrogen-content wastewater. Biodegrad. 23 (2012) 509-524. https://doi.org/10.1007/s10532-011-9529-2

[26] APHA, Standard methods for the examination of water and wastewater (22nd Ed.), American Public Health Association, Washington DC, p. 541, (2005).

[27] T. Kindaichi, T. Awata, Y. Mugimoto, R.M.L.D. Rathnayake, S. Kasahara, H. Satoh, Effects of organic matter in livestock manure digester liquid on microbial community

structure and in situ activity of anammox granules, Chemosphere 159 (2016) 300-307. https://doi.org/10.1016/j.chemosphere.2016.06.018

[28] C.G. Casagrande, A. Kunz, M.C. De Prá, C.R. Bressan, H.M. Soares, High nitrogen removal rate using ANAMMOX process at short hydraulic retention time. Water Sci. Technol. 65 (2013) 968-975. https://doi.org/10.2166/wst.2013.641

[29] T.E. Agustina, N. Novia, G. Diansyah, M. Ike, S. Soda, Nitrogen removal by anammox biofilm column reactor at moderately low temperature. Indones. J. Fundam. Appl. Chem. 2(3) (2017) 78-82. https://dx.doi.org/10.24845/ijfac.v2.i3.78

[30] Y.-m. Han, F.-x. Liu, X.-f. Xu, Z. Yan, Z.-j. Liu, Nitrogen removal via a single-stage PN–Anammox process in a novel combined biofilm reactor, Water Sci. Technol. 77 (2018) 77(6), 1483-1492. https://doi.org/10.2166/wst.2017.572

[31] N.V. Tuyen, J.H. Ryu, H.G. Kim, S.W. Hong, D.H. Ahn, Nitrogen removal performance of anammox process with PVA–SA gel bead crosslinked with sodium sulfate as a biomass carrier, J. Ind. Eng. Chem. 67 (2018) 326-332. https://doi.org/10.1016/j.jiec.2018.07.004

[32] N. Hudayah, B. Suraraksa, P. Chaiprasert, Impact of EPS and chitosan combination on enhancement of anaerobic granule quality during simultaneous microbial adaptation and granulation, J. Chem. Technol. Biotechnol. 94 (2019) 7525-3735. https://doi.org/10.1002/jctb.6180

[33] R. Yang, H. Li, M. Huang, H. Yang, A. Li, A review on chitosan- based flocculants and their applications in water treatment, Water Res. 95 (2016) 59-89. https://doi.org/10.1016/j.watres.2016.02.068

[34] I.D. Patil, M. Husain, V.R. Rahane, Ground water nitrate removal by using ‘Chitosan’ as an adsorbent, Int. J. Modern Eng. Res. 3 (2013) 346-349.

[35] M.D.G. de Luna, C.M. Futalan, C.A. Jurado Jr., J.I. Colades, M.-W. Wan, Removal of ammonium- nitrogen from aqueous solution using chitosan- coated bentonite: Mechanism and effect of operating parameters, Appl. Polym. 135 (2018) 45924. https://doi.org/10.1002/app.45924

[36] F. Almomani, R. Bhosale, M. Khraisheh, A. Kumar, T. Almomani, Heavy metal ions removal from industrial wastewater using magnetic nanoparticles (MNP), Appl. Surf. Sci. 506 (2020) 144924. https://doi.org/10.1016/j.apsusc.2019.144924

[37] S.A. Al-Saydeh, M.H. El-Naas, S.J. Zaidi, Copper removal from industrial wastewater: A comprehensive review, J. Ind. Eng. Chem. 56 (2017) 35-44. https://doi.org/10.1016/j.jiec.2017.07.026

[38] X. Zhang, Y. Zhou, N. Zhang, K. Zheng, L. Wang, G. Han, H. Zhang, Short-term and long-term effects of Zn (II) on the microbial activity and sludge property of partial nitrification process, Bioresour. Technol. 228 (2017) 315-321. https://doi.org/10.1016/j.biortech.2016.12.099

[39] A. Mojiri, K. Nishimoto, T. Awata, Y. Aoi, N. Ozaki, A. Ohashi, T. Kindaichi, Effects of salts on the activity and growth of "*Candidatus scalindua* sp.", a marine anammox bacterium, Microbes and Environ. 33 (2018) 336-339. https://doi.org/10.1264/jsme2.ME18068

[40] T. Lotti, M. Cordola, R. Kleerebezem, S. Caffaz, C. Lubello, M.C.M. van Loosdrecht, Inhibition effect of swine wastewater heavy metals and antibiotics on anammox activity, Water Sci. Technol. 66 (2012)1519-1526. https://doi.org/10.2166/wst.2012.344

[41] Y. Liu, B.J. Ni, Appropriate Fe (II) addition significantly enhances anaerobic ammonium oxidation (anammox) activity through improving the bacterial growth rate, Sci. Rep. 5 (2015), 8204. https://doi.org/10.1038/srep08204

[42] M.S. Rana, M.A. Halim, S. Safiullah, M.M. Mollah, M.S. Azam, M.A. Goni, M.K. Hossain, M.M. Rana, Removal of heavy metal from contaminated water by biopolymer crab shell chitosan, J. Appl. Sci. 9 (2009) 2762-2769. https://doi.org/10.3923/jas.2009.2762.2769

[43] N.A. Reiad, O.E. Abdel Salam, E.F. Abadir, F.A. Harraz, Adsorptive removal of iron and manganese ions from aqueous solutions with microporous chitosan/polyethylene glycol blend membrane, J. Environ. Sci. 24 (2012) 1425-1432. https://doi.org/10.1016/S1001-0742(11)60954-6

Getting biomass and homogenizing

Pouring the homogenized liquid to the first reactor

Growing anammox bacteria in the first reactor

Figure 1:

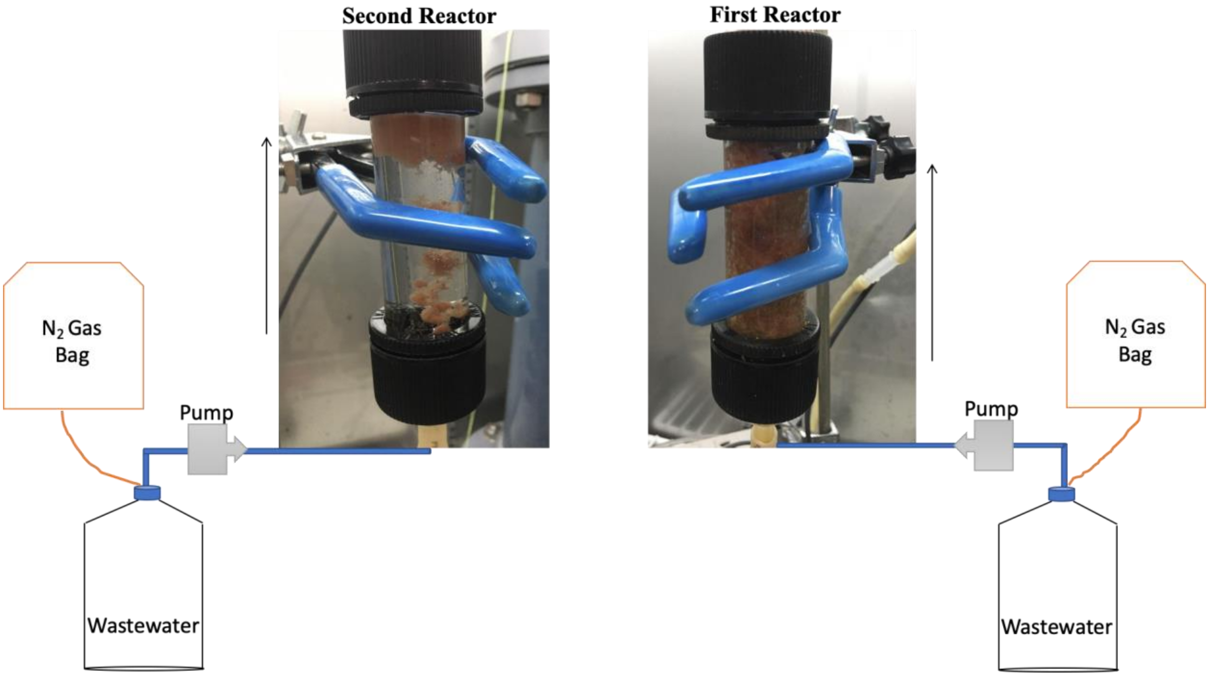
Second Reactor
First Reactor
N2 Gas
Bag
Pump
Wastewater
Pump
N2 Gas
Bag
Wastewater

Figure 2:

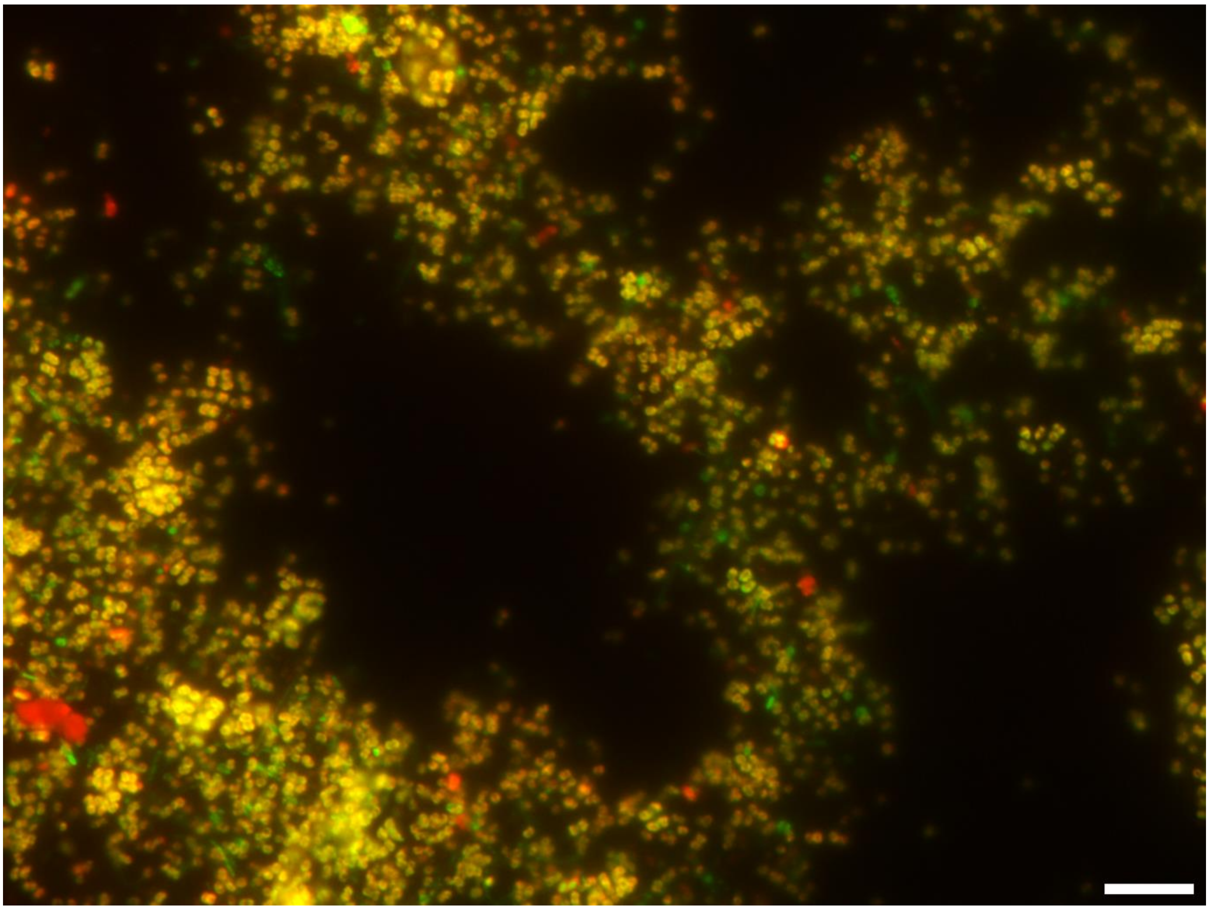

Figure 3:

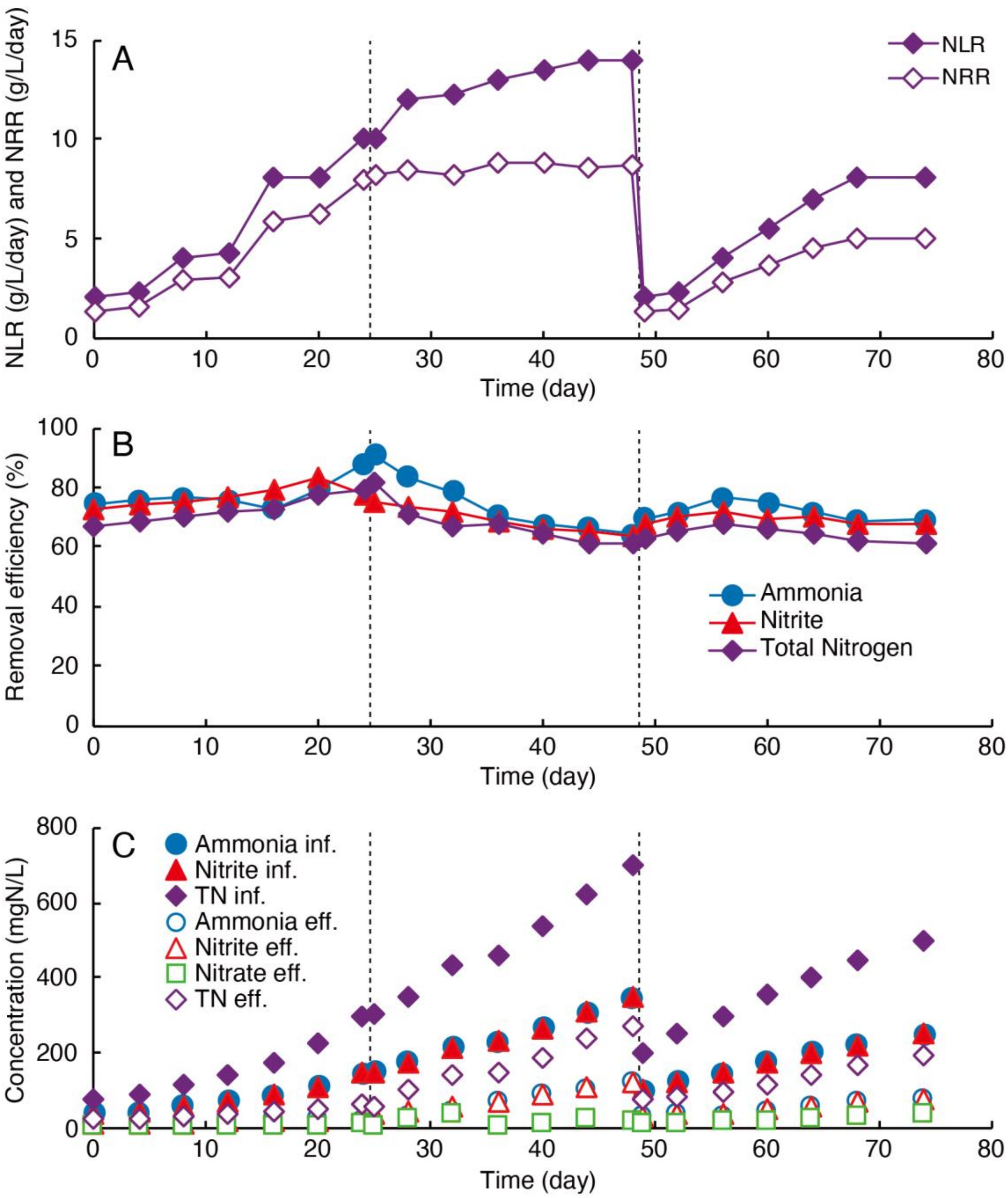
A
NLR
NRR
NLR (g/L/day) and NRR (g/L/day)
Time (day)
B
Removal efficiency (%)
Ammonia
Nitrite
Total Nitrogen
Time (day)
C
Concentration (mgN/L)
Ammonia inf.
Nitrite inf.
TN inf.
Ammonia eff.
Nitrite eff.
Nitrate eff.
TN eff.
Time (day)

Figure 4:

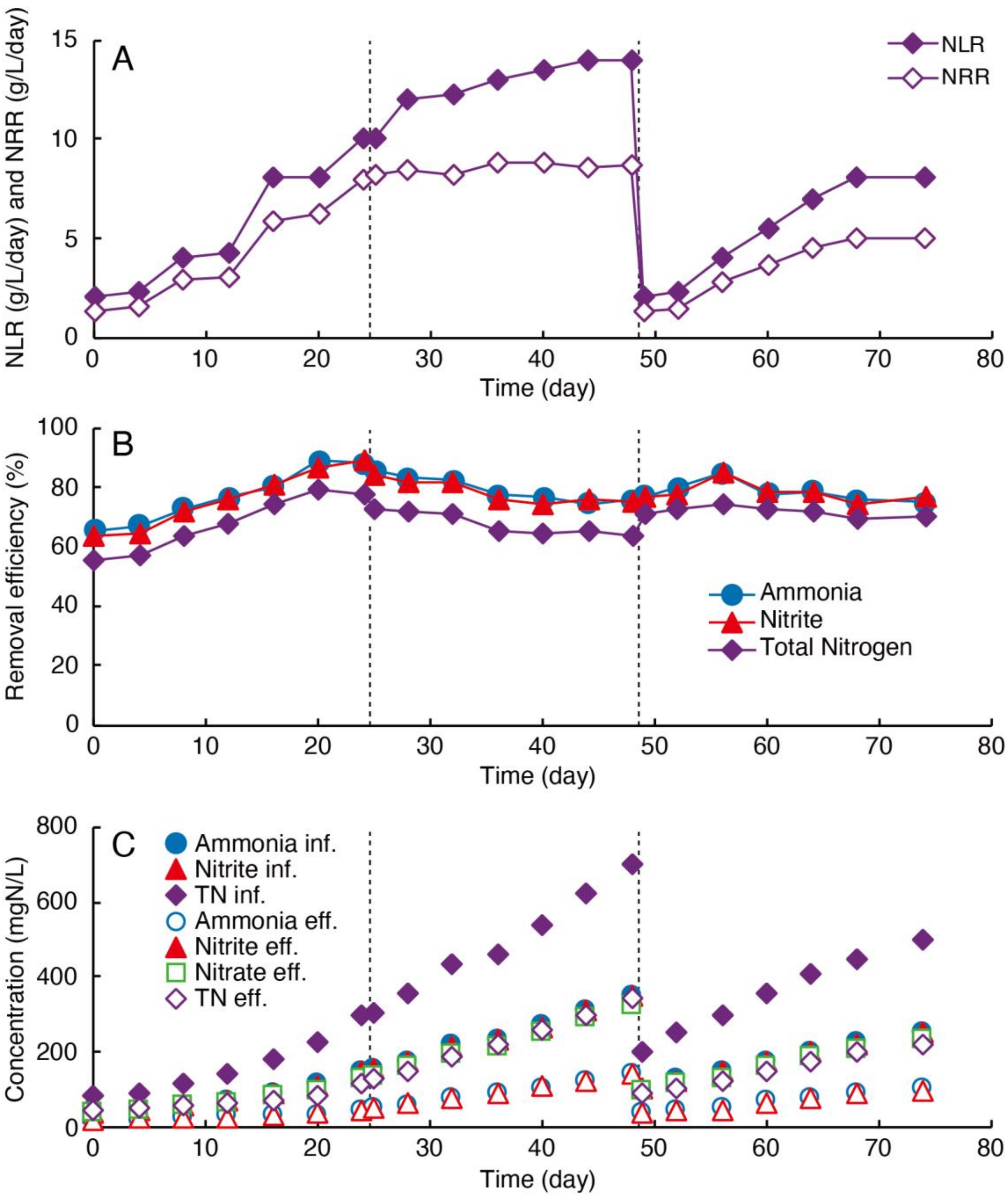

A
NLR
NRR
NLR (g/L/day) and NRR (g/L/day)
Time (day)
B
Removal efficiency (%)
Ammonia
Nitrite
Total Nitrogen
Time (day)
C
Concentration (mgN/L)
Ammonia inf.
Nitrite inf.
TN inf.
Ammonia eff.
Nitrite eff.
Nitrate eff.
TN eff.
Time (day)

Figure 5:

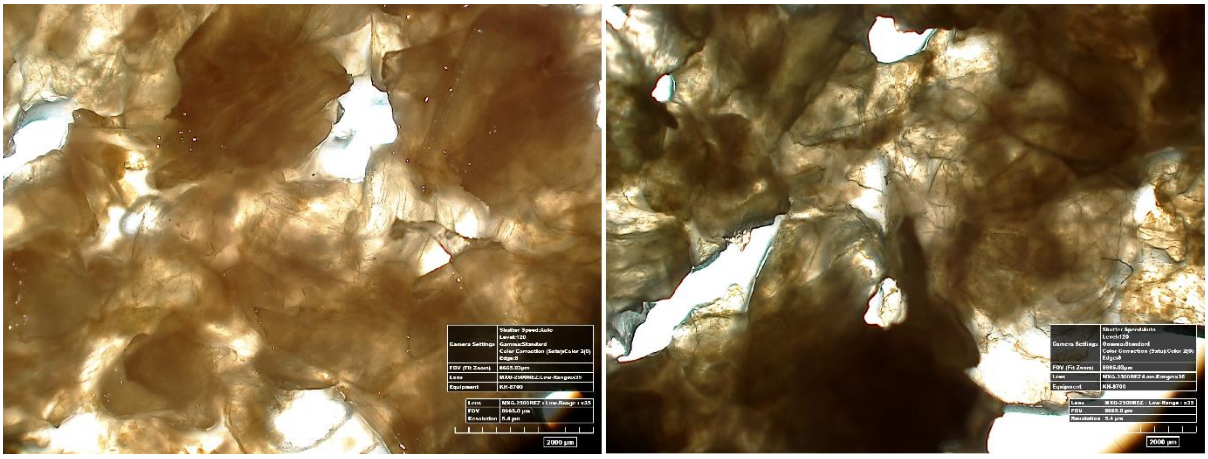
Camera Settings
Shutter Speed:Auto
Level:120
Gamma:Standard
FOV (Fit Zoom)
Lens
Equipment
Lens
FOV
8665.0 µm
Resolution
2000 µm

Figure 6:

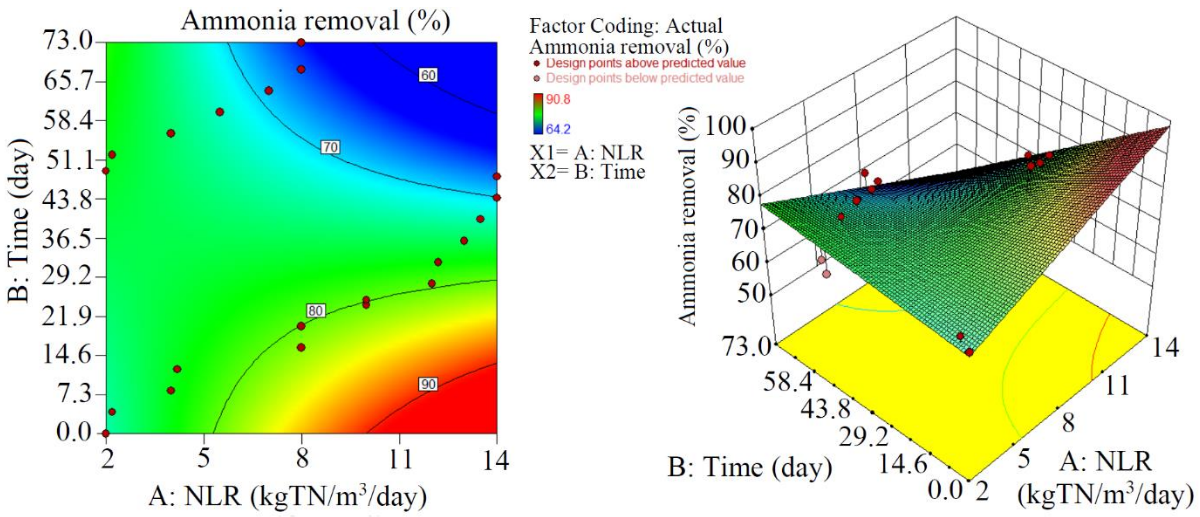
Ammonia removal (%)
B: Time (day)
A: NLR (kgTN/m³/day)
73.0
65.7
58.4
51.1
43.8
36.5
29.2
21.9
14.6
7.3
0.0
2
5
8
11
14
60
70
80
90
Factor Coding: Actual
Ammonia removal (%)
Design points above predicted value
Design points below predicted value
90.8
64.2
X1= A: NLR
X2= B: Time
Ammonia removal (%)
100
50
(kgTN/m³/day)

(A)

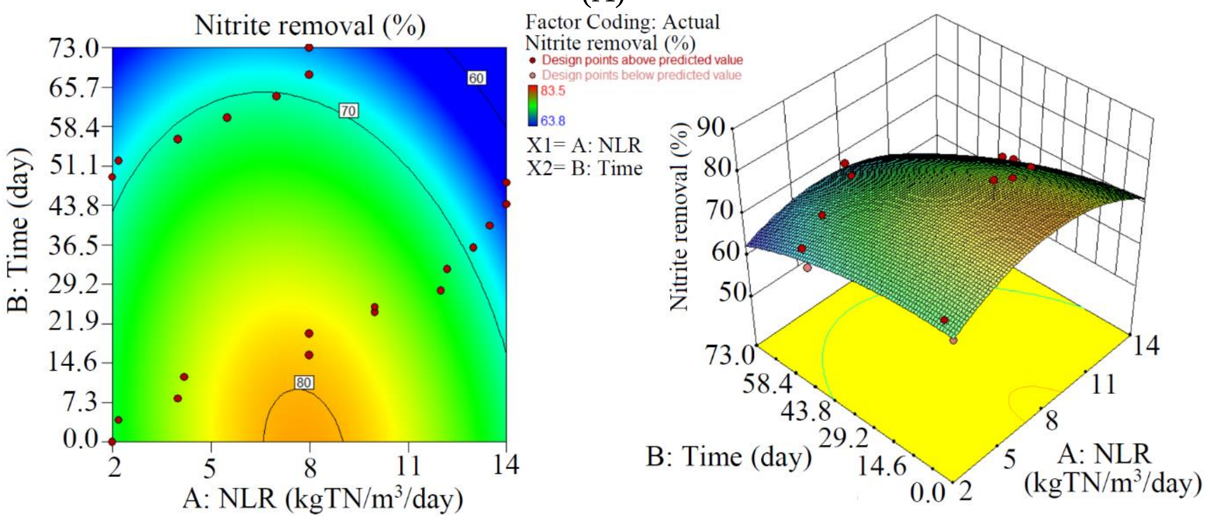
Nitrite removal (%)
B: Time (day)
A: NLR (kgTN/m³/day)
60
70
80
Factor Coding: Actual
Nitrite removal (%)
Design points above predicted value
Design points below predicted value
83.5
63.8
X1= A: NLR
X2= B: Time
Nitrite removal (%)
(kgTN/m³/day)

(B)

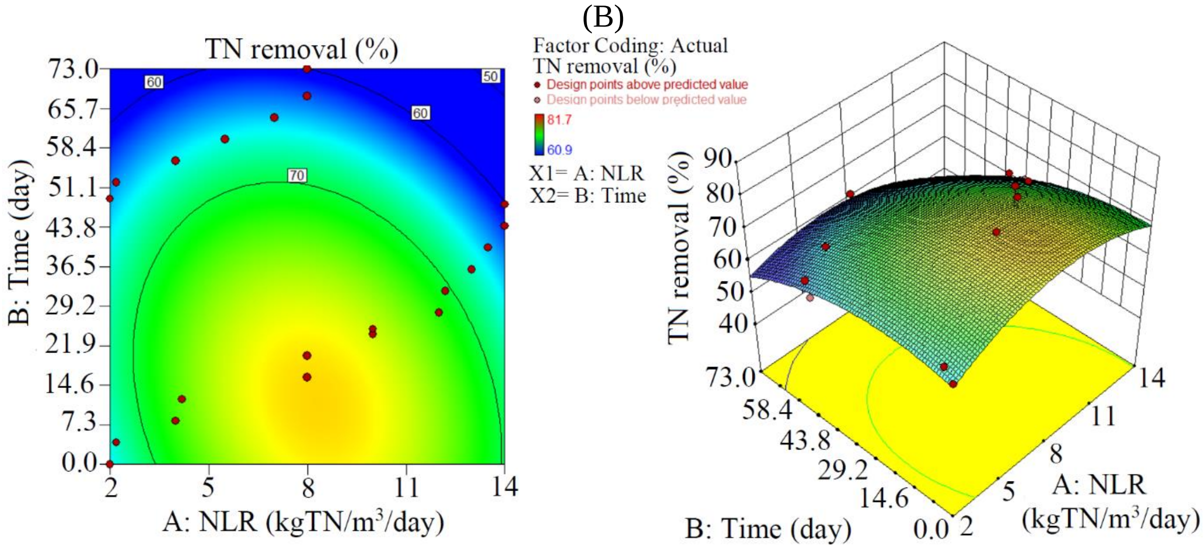
TN removal (%)
B: Time (day)
A: NLR (kgTN/m³/day)
50
60
70
Factor Coding: Actual
TN removal (%)
Design points above predicted value
Design points below predicted value
81.7
60.9
X1= A: NLR
X2= B: Time
TN removal (%)
(kgTN/m³/day)

(C)

Figure 7:

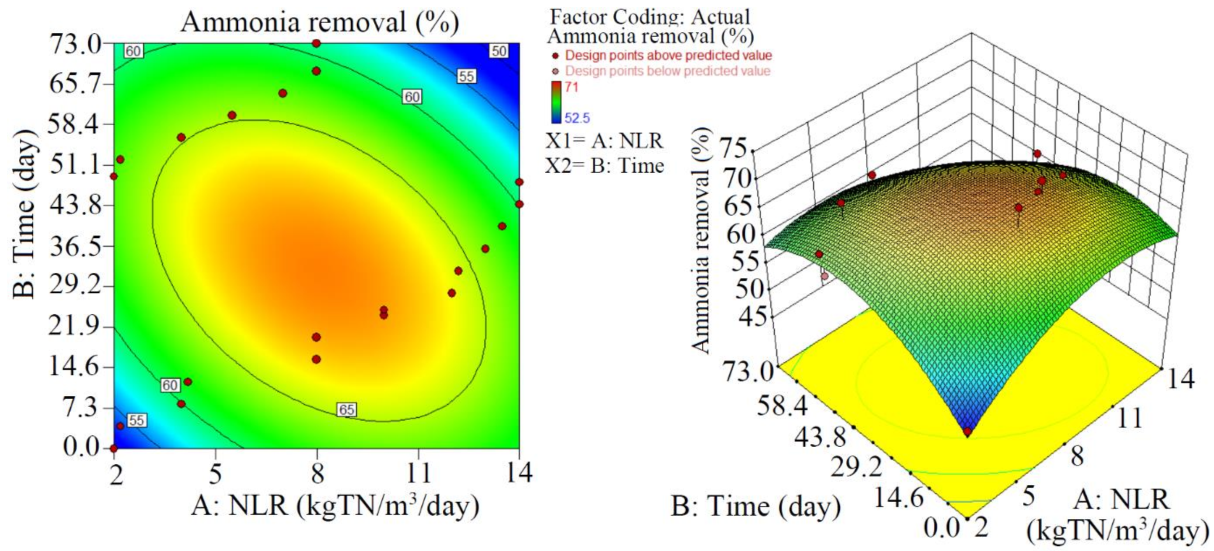
Ammonia removal (%)
B: Time (day)
A: NLR (kgTN/m³/day)
Factor Coding: Actual
Ammonia removal (%)
Design points above predicted value
Design points below predicted value
71
52.5
X1= A: NLR
X2= B: Time
Ammonia removal (%)

(A)

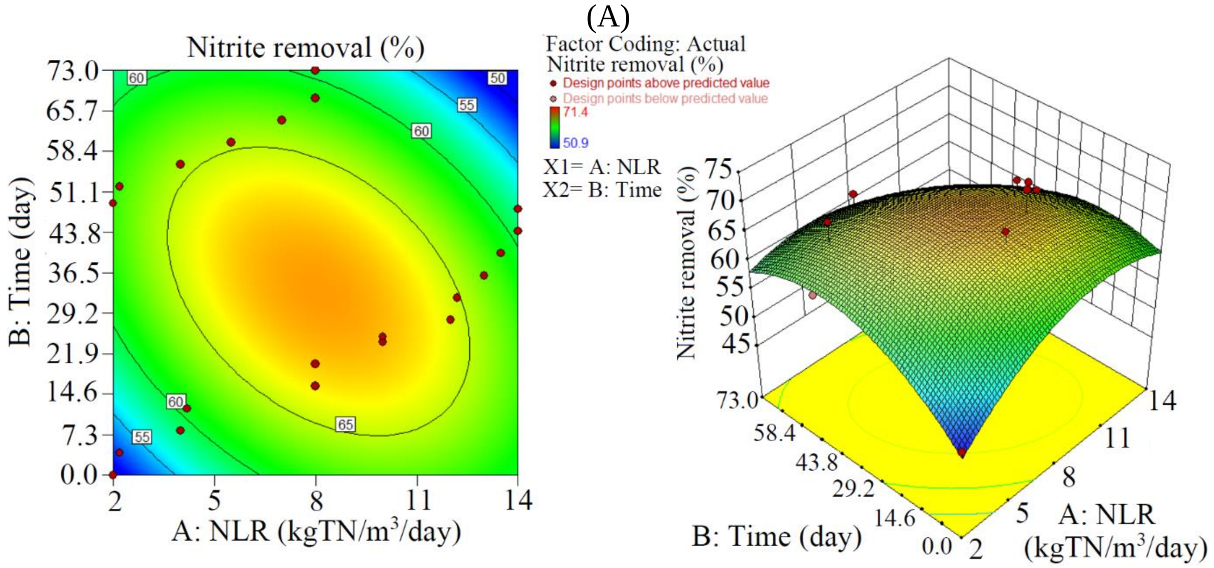
Nitrite removal (%)
B: Time (day)
A: NLR (kgTN/m³/day)
Factor Coding: Actual
Nitrite removal (%)
Design points above predicted value
Design points below predicted value
71.4
50.9
X1= A: NLR
X2= B: Time
Nitrite removal (%)

(B)

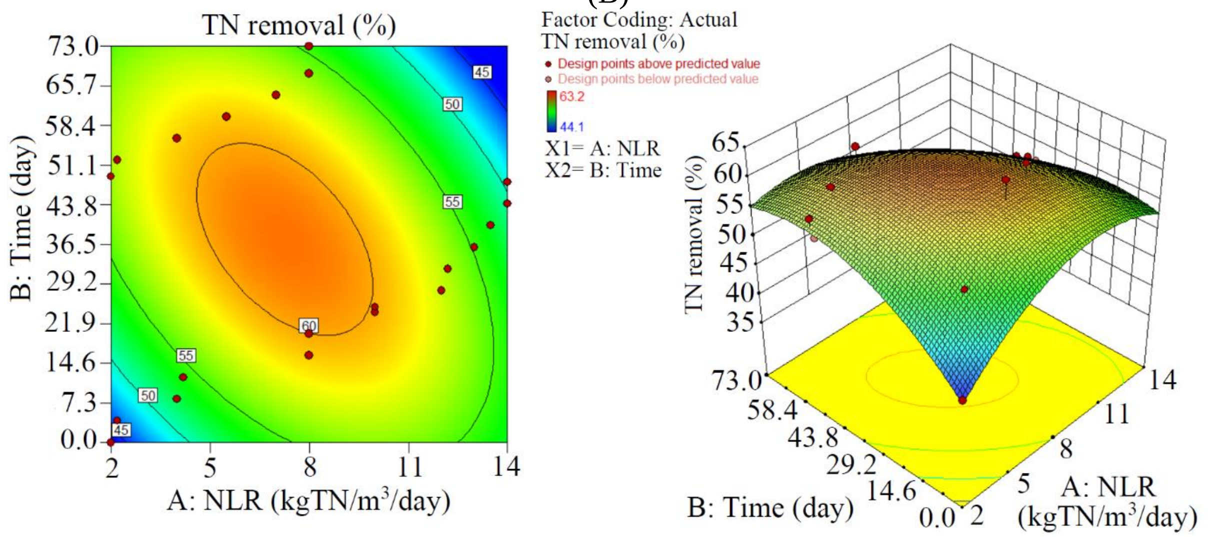
TN removal (%)
B: Time (day)
A: NLR (kgTN/m³/day)
Factor Coding: Actual
TN removal (%)
Design points above predicted value
Design points below predicted value
63.2
44.1
X1= A: NLR
X2= B: Time
TN removal (%)

(C)

Figure 8:

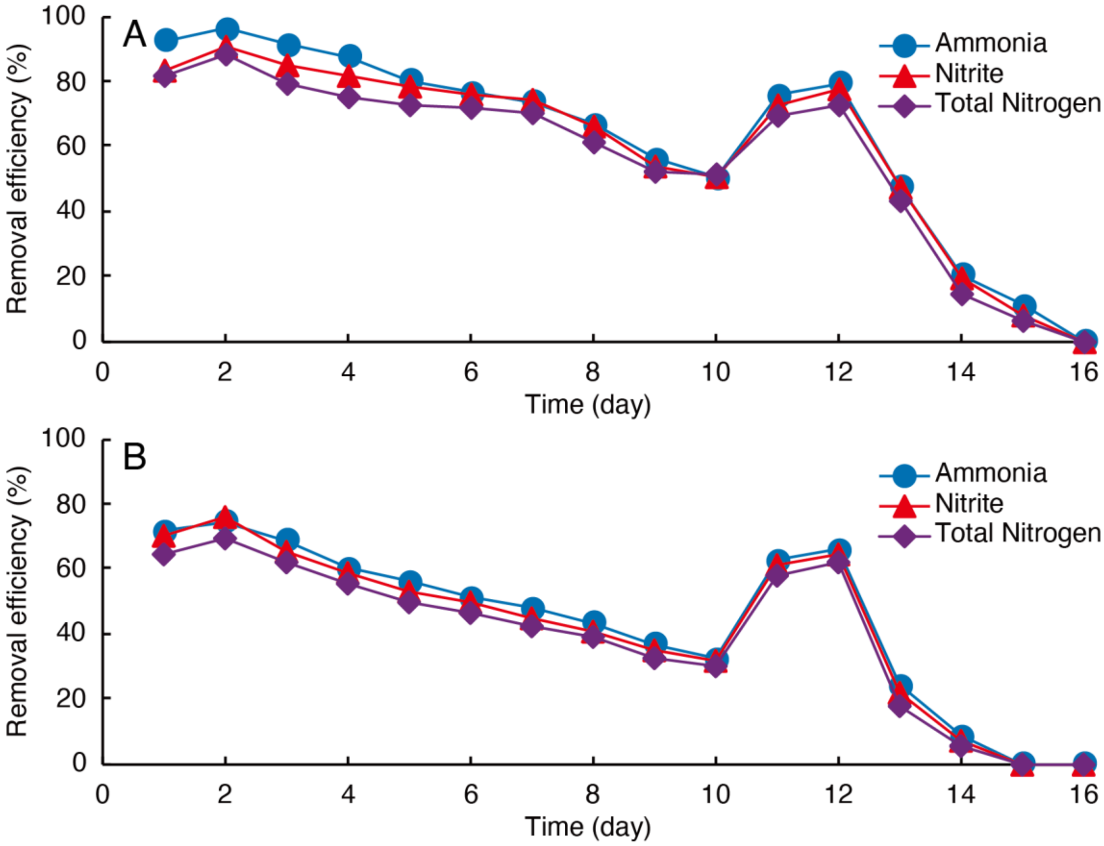

A
B
Removal efficiency (%)
Time (day)
Ammonia
Nitrite
Total Nitrogen
0
20
40
60
80
100
2
4
6
8
10
12
14
16

Figure 9:

Tables:

Table 1: Table 1: Fixed conditions during the reactor runs

Table 2: Statistical analysis results for the response parameters in the response surface methodology (RSM)

Table 3: Removal efficiencies under optimum conditions

Table 4: Addition of different concentrations of Fe and Cu in the reactors

Table 5: Langmuir and Freundlich isotherm studies for ammonia, Fe, and Cu removal by chitosan

Table 1:

Phases	Period (day)	Temperature (∘C)	Influent ammonia (mg/L)	Influent nitrite (mg/)	N loading rate (kg/TN/m^3/day)
1	0-24	24±2	40 – 150	40 - 150	2 – 10
2	25-48	24±2	150 - 350	150 - 350	10 – 14
3	49-73	24±2	100 - 250	100 - 250	2 - 8

Average of hydraulic retention time was 1.2 h

Table 2:

Reactors	Responses	**Optimization with RSM**				**Final equation in terms of actual factor**
		R^2*	**Adj. R^2**	**Adec. P.**	**SD**	
Reactor-1	TN	0.85	0.80	12.16	2.64	$58.50 + 0.22B – 0.24A^2$
	Ammonia	0.81	0.78	7.08	5.26	$68.72 + 0.19B – 0.59AB$
	Nitrite	0.91	0.89	18.74	1.63	$66.50 + 0.5B – 0.22A^2$
Reactor-2	TN	0.91	0.88	18.60	1.65	$36.40 – 0.19A^2$
	Ammonia	0.86	0.82	15.86	1.98	$44.62 – 0.17A^2$
	Nitrite	0.86	0.82	15.71	2.12	$42.61 – 0.19A^2$

*R^2: Coefficient of determination; Adj. R^2: Adjusted R^2; Adec. P.: Adequate precision; SD: Standard deviation; and MSE: mean squared errors

A: time (day); B: nitrogen loading rate (kgTN/m^3/day)

Table 3:

Reactors	NLR (kgTN/m^3/day)	Time (day)	TN removal (%)	Ammonia removal (%)	Nitrite removal (%)
1	9.6	14.5	76.5	89.3	79.6
2	7.7	33.8	61.0	68.7	68.3

Table 4:

Runs	Metals concentrations (mg/L)
1	0.5
2	1.0
3	1.5
4	2.0
5	2.5
6	3.0
7	3.5
8	4.0
9	4.5
10	5.0
11	1.0
12	1.0
13	5.5
14	6.0
15	6.5
16	7.0

Table 5:

Parameters	Langmuir Isotherm			Freundlich Isotherm		
	Q_0 (mg/g)	b	R^2	K_f (mg/g(L/mg)$^{1/n}$)	1/n	R^2
Ammonia	0.28	0.19	0.83	16.2	0.06	0.93
Fe	0.11	0.21	0.81	0.9	0.83	0.85
Cu	0.21	0.23	0.84	5.3	0.37	0.89